Circumferential failures in grey cast iron pipes
Makar, J. M.; Rogge, R.; McDonald, S. E.

Circumferential failures in grey cast iron pipes

Makar, J.M.; Rogge, R.; McDonald, S.E.

NRCC-45013

A version of this paper is published in / Une version de ce document se trouve dans:
2002 AWWA Infrastructure Conference, Chicago, March 10-13, 2002, pp. 1-18

Circumferential Failures in Grey Cast Iron Pipes

Jon Makar*, Ph.D., P. Eng.
Institute for Research in Construction

Ron Rogge, Ph.D.
Neutron Program for Materials Research

Shelley McDonald, P. Eng.
Institute for Research in Construction

National Research Council Canada
1200 Montreal Road, Ottawa, Ontario K1A 0R6
Canada

1 Introduction

Circumferential cracking (Figure 1) may be responsible for up to 80% of the failures in small diameter (<200 mm / 8 in), grey cast iron water mains (Rajani and McDonald, 1995). However, while failures due to crushing and internal water pressure are well understood and discussed in the relevant manufacturing standards (AWWA, 1939; 1953), circumferential failures have not been investigated in detail. Although Talbot showed that circumferential failures are produced by pipe bending (Talbot, 1926), no modern studies appear to have been performed. In particular, the effect of corrosion pits and graphitisation on circumferential failures is not well understood. While studies (Makar, Desnoyers and McDonald, 2001) have shown that more than 90% of the circumferential failures have been associated with the presence of a corrosion pit at the failure surface, the effect of a corrosion pit of a particular size and depth on the residual strength of a grey cast iron pipe remains unknown.

Despite this lack of knowledge, the last decade has seen the development of non-destructive testing techniques that can measure the depth of corrosion pitting in in-service cast iron pipes (Makar and Chagnon, 1999). Sampling programs to estimate the quality of gray cast iron pipes and procedures for estimating the remaining service life of grey cast iron pipes have also been developed (Rajani and Makar, 2000). The goal of these developments is to enable water utilities to better manage their distribution systems, repairing and replacing them in the most economical manner possible.

*Corresponding author – email: jon.makar@nrc.ca

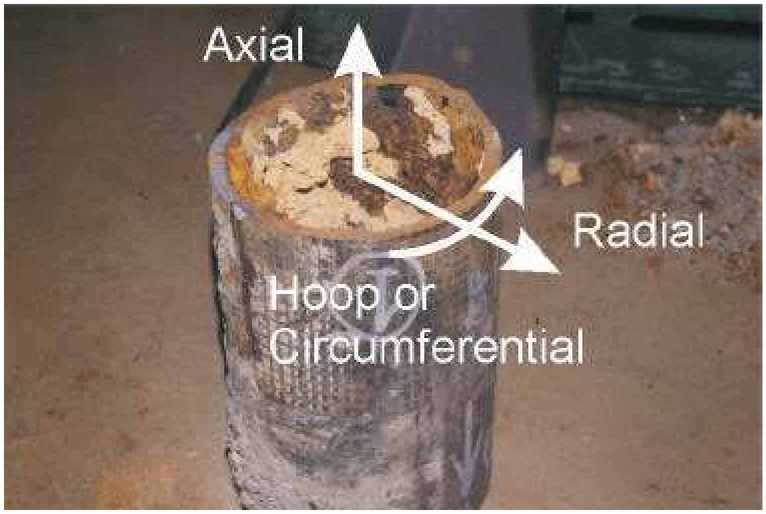

Figure 1 - An example of a circumferential failure, showing the reference directions used in the text

Interpreting the results from the different techniques and procedures requires a clear understanding of the mechanical behaviour of in-service pipes. This knowledge is essential for relating field measurements or estimates of corrosion pit depth to the risk of a pipe failure. Understanding the connections between corrosion pitting, the loads experienced by in-service pipes, the pipe material and the risk of circumferential failure should assist water utilities in making better pipe management decisions.

This paper describes an American Water Works Association Research Foundation funded research project "Circumferential Failures in Grey Cast Iron Distribution Pipes" currently underway at the National Research Council Canada (NRC) to investigate circumferential failures under a wide variety of loading and soil conditions. It combines mechanical testing of pipe coupons, experimental measurements of pipes in bending using the *neutron diffraction* method and finite element modeling. Neutron diffraction can measure the strain distribution around a corrosion pit in a pipe that is in bending, while finite element modeling can be used to determine investigate how changing soil and loading conditions affect pipe failures. Combining the two techniques gives the potential to produce an accurate understanding of the conditions that cause circumferential failures and to determine when a corrosion pit becomes a threat to the integrity of a water pipe.

The project involves three different phases: uniaxial mechanical testing of coupons taken from pipe samples, neutron diffraction measurements on pipe samples in bending and finite element modeling. The uniaxial mechanical testing is intended to provide appropriate stress-strain curves and Poisson's ratio data for the cast iron pipe samples used in the project for use as inputs to the finite element modeling phase. Section 3 of this paper describes results from the mechanical testing phase. The neutron diffraction measurements show the strains in bent sections of pipe as well as whole pipe sections. These measurements will be used to provide a check on the validity of the finite element models and to ensure that the mechanical behaviour of grey cast iron in the triaxial stress states found in bending pipes is fully undertstood. The finite element models will need to duplicate the experimentally observed behaviour before modeling of pipes in soil begins. Section 4 of the paper shows some of the first neutron diffraction results from the project. Finally, future work on finite element modeling will investigate the interaction between the pipes, corrosion pits and the surrounding environmental conditions. It should provide guidance on the potential for premature pipe failure due to corrosion pits of different sizes and dimensions.

2 Neutron Diffraction

2.1 Neutrons

Neutrons are a subatomic particle most frequently found as part of the nucleus of almost all atoms. The most common form of helium has two neutrons and two protons in its nucleus, the most common form of carbon has six of each type of subatomic particle, while the most common form of iron has 36 neutrons and 20 protons. Neutrons and protons have approximately the same size and mass, but a neutron is electrically neutral with no charge, while a proton has a charge of $+1.6 \times 10^{-19}$ C. (Electrons, which orbit around the nucleus of an atom, each have a negative charge of -1.6×10^{-19} C.)

While neutrons are generally found inside atomic nuclei, they can also be emitted from those nuclei when they are struck by another atomic or subatomic particle. One way of producing neutrons is through the use of a nuclear reactor. When a neutron hits an atom of uranium that has the right number of neutrons (U^{238}, with 92 protons and 146 neutrons), the atom undergoes a fission process, producing two smaller atoms, heat and more neutrons. The new neutrons are slowed down by passing through a moderator material such as light or heavy water. They are then available to hit other atoms, continuing the reaction. The heat from the continuing reaction is used to generate electricity.

Nuclear reactors are surrounded by shielding to prevent the radiation and particles (such as neutrons) produced inside the reactor from escaping to the outside environment. However, it is possible to design the reactor to allow for the controlled emission of neutrons through the shielding. These neutrons can then be used for different types of materials research and engineering. Examples include the measurement of stresses, chemical phase analysis, investigations of crystal structure, structural chemistry and the investigation of biological materials. One of the major advantages of neutron based research is that the techniques are generally non-destructive, which means that the samples can be analysed using a neutron technique and still be available for further testing using other techniques.

2.2 Neutron Diffraction

One of the major applications for neutrons is neutron diffraction (Lu, 1996; Noyan and Cohen, 1987). This technique sends a beam of neutrons into a crystalline material. The wavelength of the beam of neutrons has a size that is of the same order of magnitude as the distance between the atoms in the crystalline material, making the beam a good probe for properties that depend on the atomic spacing. In neutron diffraction, the beam "diffracts" by interacting with the lattice of atoms in the crystal. Diffraction refers to the process of bending the beam of neutrons as whole through the scattering of the neutrons from individual atomic nuclei in the crystal. Figure 2 illustrates the diffraction process.

The angle, 2θ, at which neutrons diffract from the crystal lattice inside a sample depends on the wavelength of the incident neutron beam, λ, and the spacing between the lattice planes, d, through Bragg's law,

$$\lambda = 2d\sin(\theta)\,. \tag{1}$$

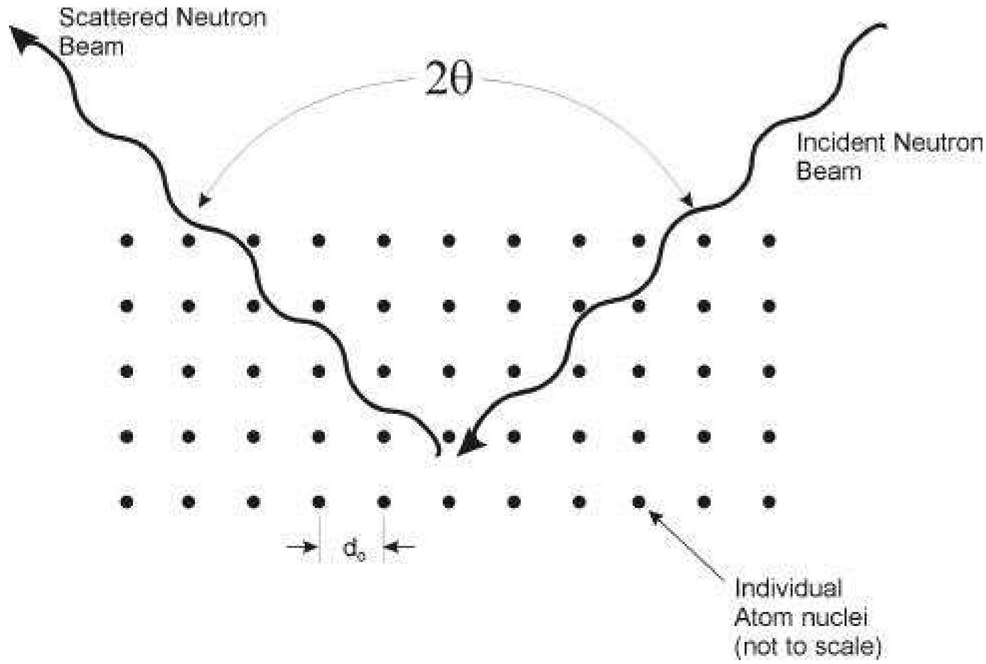

Figure 2 – Neutron Diffraction

The lattice strain, ε, is the fractional change in the lattice spacing with reference to the *stress-free* lattice spacing, d_o, with

$$\varepsilon = \frac{d - d_o}{d_o}. \quad (2)$$

Measuring the angle of diffraction can therefore produce a measurement of the lattice strain. The measured strain is along the vector that bisects the vectors of the incident and scattered neutron beams (the beams are the black lines in Figure 3). Re-orienting the sample being investigated allows the researcher to measure strains in different directions. Measurements in three perpendicular directions can therefore give the three dimensional strain distribution in the sample. The beam of neutrons measures the strain in a sampling volume of approximately 3.5 mm^3 (2.1 x 10^{-4} in^3). The beam is also very penetrating and can make measurements through approximately 25 mm (1 in) of steel or cast iron.

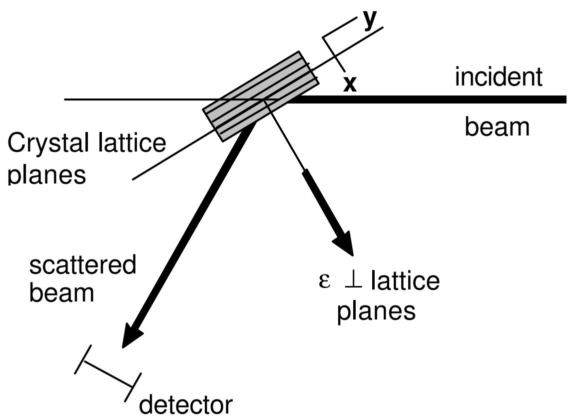

Figure 3 – Orientation of the sample and direction of measured strain

There are number of advantages to using neutron diffraction over other strain measurement techniques. Both strain gauges and x-ray diffraction only produce measurements at the surfaces of samples. Strain gauges can only produce two dimensional strain information. Measurements of residual stress using strain gauges also require damaging the sample. Neutron diffraction measures strains in a smaller area than that covered by most strain gauges. Finally, neutron diffraction measurements are non-contact in nature. Measurements can be taken from the outside of environmentally controlled boxes or on moving objects. These advantages have caused neutron diffraction to be used to investigate a variety of strain related problems, ranging from work on gas pipeline steel through investigations of operating jet engines to the analysis of components from the failure of the space shuttle Challenger.

3 Mechanical Testing Results

3.1 Stress Strain Test Results

Figure 4 shows the results of a series of tensile tests performed on coupons taken from a single spun cast pipe. The coupons were cut to shape from the pipe wall, following ASTM standard E8 (specimen shape 1 on page 9 of the standard; ASTM 1994). As permitted by the standard, the outside and inside surfaces of the coupons remained curved, rather than being flattened and the tensile tests were done using a curved set of grips. The strains in these tests were measured by the use of an extensometer, which is also permitted in the standard. As can be seen in Figure 4, the results were highly variable. This degree of variability does not reflect the behaviour that would be expected for this material from the literature (Walton and Opar, 1981).

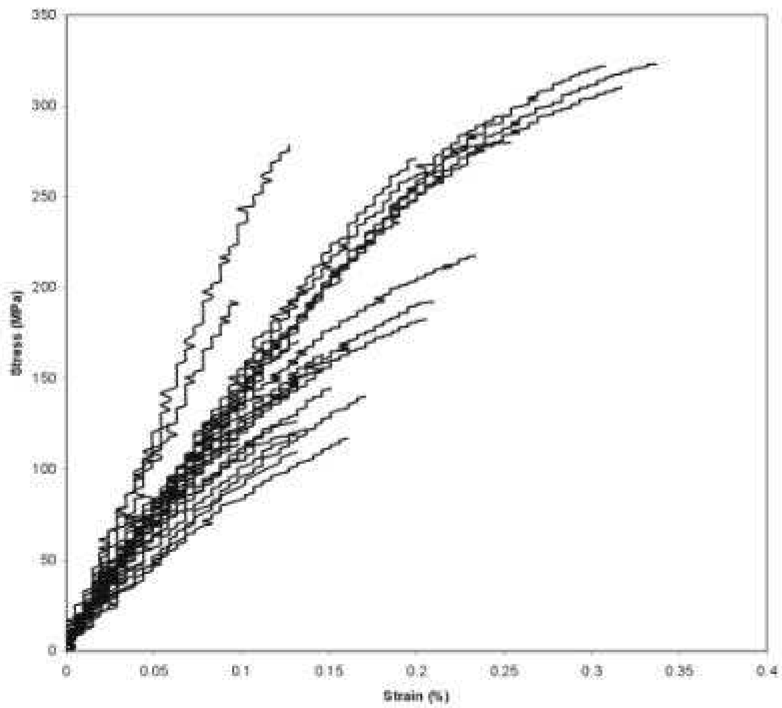

Figure 4 - Stress-strain results from a single pipe using curved samples

Further investigations were made with curved samples that had been instrumented on their front and back with strain gauges. Figure 5 compares the readings of the two gauges to each other. Identical readings should follow the line labeled as “1 to 1” in the figure. Instead, the curved samples produced the lower, curved line in Figure 5, indicating a considerable degree of bending was taking place in the sample. While it may be difficult to avoid some degree of bending during a tensile test, the amount of bending shown is high enough to produce the variability in the stress-strain curves in Figure 4.

In contrast, Figure 6 shows a series of stress-strain curves measured on flat coupons taken from a single pipe. These coupons had the same dog bone shape as those in Figure 6, but had their surfaces milled flat. Some of the coupons were further thinned down to remove some or all of the corrosion pitting on the coupon surface. As was the case for the curved coupons, most of the strains shown in the figure were measured using an extensometer. The figure also shows a result for a strain gauge measurement, which produced a stress-strain curve similar to those measured using the extensometer.

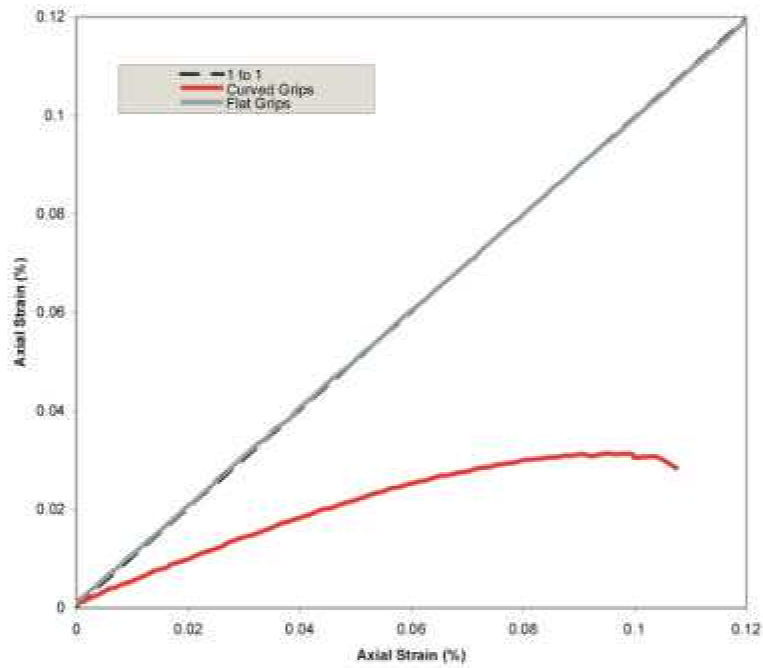

Figure 5 - Strain gauge results from curved and flat coupons

3.2 Effects of Corrosion Pits

Some of the measurements shown in both Figures 4 and 6 were performed on coupons that had corrosion pitting in their gauge length. In the tests shown in Figure 4, the corrosion pits appeared to contribute to the divergence of the stress-strain curves, as many of the curves at the left side and at the bottom of the graph had corrosion pits at the point of failure. In both the tests shown in Figure 6 and those done on coupons from other pipes, the major effect of the corrosion pits appeared to be premature failure. These results used flat coupons and the presence of the corrosion pits did not alter the slopes of the stress-strain curves, but did lower the coupons' ultimate strength and strain.

Corrosion pits in grey cast iron pipe are typically filled with graphitisation products. This material combines the graphite flake matrix found in grey cast iron with iron oxide corrosion products. Additional oxidation products from elements such as magnesium or calcium in the surrounding soil can also be found when graphitisation is chemically analysed. Graphitisation can completely fill a corrosion pit, making detection of pipe corrosion by visual examination difficult or impossible.

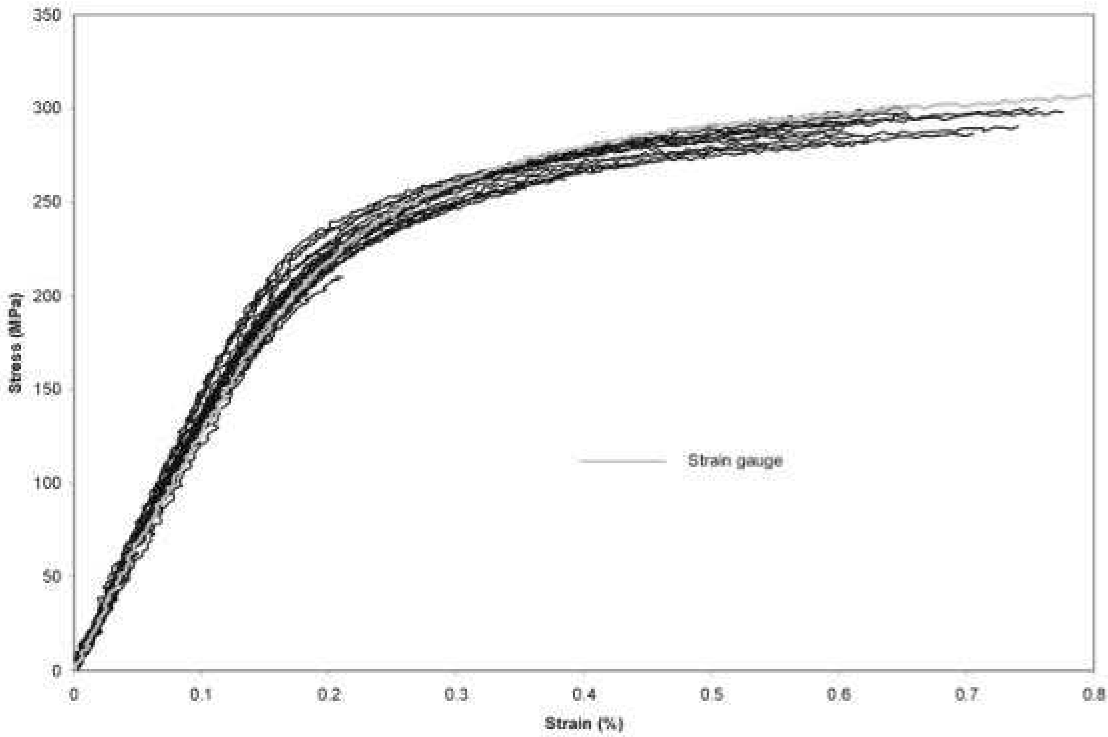

Figure 6- Stress-strain curves for flat samples

However, as shown in Figure 7, the interface region between the graphitisation products and the uncorroded metal of the pipe is very rough. This roughness may explain the impact of corrosion pits on the stress strain curves discussed above. In the case of both types of sample, areas of the interface may be acting as a crack former, providing stress concentrations that cause the early failure of the coupons. In addition, corrosion pits can extend most or all of the way through a pipe wall. The presence of a corrosion pit in a sample that is already undergoing bending may accelerate the bending process by altering the neutral axis of the coupon and therefore changing its stress distribution. It will also produce an additional stress concentration effect related to the bending (Beer and Johnston, 1981). Further work will be needed to confirm these effects in the pipe samples.

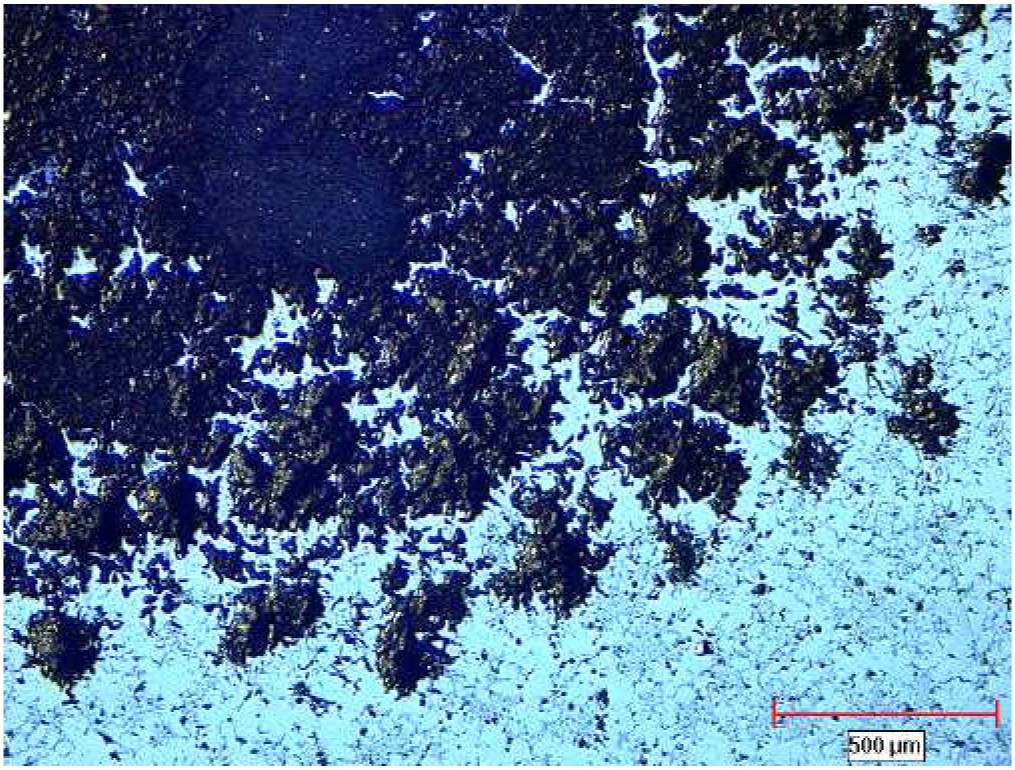

Figure 7 - Interface region between graphitisation (dark material) and uncorroded metal in cast iron

3.3 Guidance on stress testing coupons from gray cast iron pipes

In addition to the problems noted above, there are at least two other potential sources of error that need to be accounted for in the testing of gray cast iron pipes that may have been corroded. First, the presence of corrosion pits in the area of the sample under the grips may cause slipping of the sample or promote bending, depending on the size and location of the pit. Secondly, the use of extensometers can be problematic if an arm of the extensometer rests against a corrosion pit or scratches the coupon. In the first case, the arm may slip along or dig into the graphitisation product that fills the corrosion pit, rendering the measurement of the strain inaccurate. In the second case, the scratch may promote a premature failure in the sample. Failures were not created by scratches produced by the extensometer arms in the coupons tested for the work presented here, but ASTM E8 notes that scratches need to be removed from the surface of tensile samples made from brittle materials in order to avoid this type of failure.

Based on the results presented here, practitioners may find the following points a useful extension of ASTM E8 as guidance on testing of gray cast iron samples:

- Flat coupons are significantly more likely to provide accurate results than curved samples;
- Cutting a strip from a pipe and removing the outer and inner surfaces in order to flatten it will reveal any surface pitting that can not be identified from the sides of the strip. Test coupons can then be located along the strip so that material that would be under the grips does not have corrosion pitting;
- Corrosion pits along the gauge length are likely to cause premature failure of uniaxial test samples. If possible, at least some tests should be done on samples without corrosion pitting;
- Multiple coupons should be taken from any given pipe that will be tested in order to provide a check on the validity of the tests;
- Extensometers should be used with care and their results checked by strain measurements made with strain gauges;
- As much of the full thickness of a pipe wall as possible should be used to produce the flat samples. In some cases, the microstructure of the pipe material will change across the pipe wall, causing the material's strength to vary across the wall as well; and
- Samples should be strain gauged on two sides to check for bending.

It is particular important that the guidance of ASTM E8 with respect to removing scratches from the gauge length of brittle samples should be followed.

Finally, it should be noted that the effects of the corrosion pits on the failure of the uniaxial stress-strain coupons may not reflect their effects on the failure of the pipes themselves. As discussed in Section 4.2, the uniaxial stress-strain results are not necessarily the same as those observed under the triaxial stress conditions observed for a pipe in bending.

4 Initial Neutron Diffraction Results

4.1 Neutron Diffraction Apparatus

Figure 8 shows one of the two stress rigs used during the neutron diffraction experiments. In the figure, the incident neutron beam is coming from the drum on the right hand side of the picture, entering the pipe section and then diffracting to travel to a detector at the end of box shown at the front of the picture.

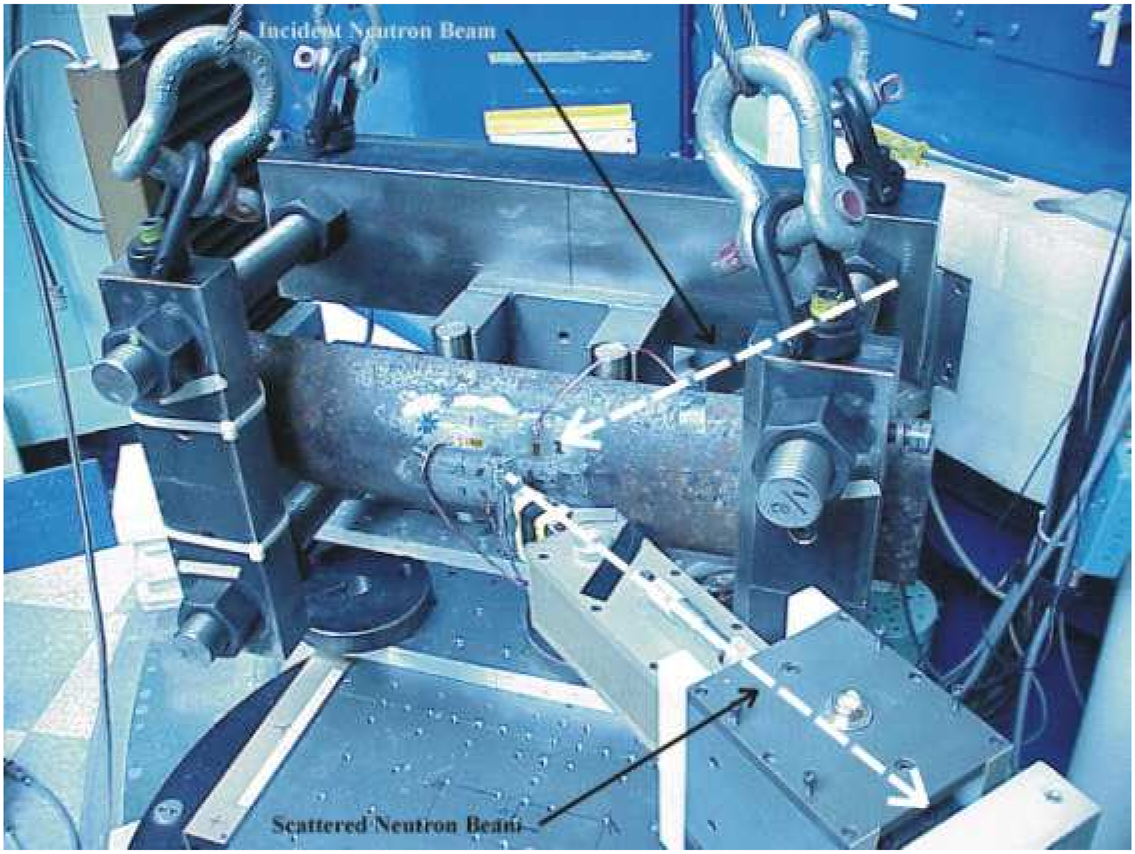

Figure 8 - Short test rig showing an axial strain measurement on a pipe section

The short rig in the picture is bending a section of a 150 mm (6”) diameter pipe that covers one third of the circumference of a full pipe. The measurement arrangement shown is used to take measurements of the axial strain. Measurements of the hoop strain (see Figures 1 and 9) are taken with the rig rotated so that the outer surface of the pipe section is facing up, while radial measurements are taken with the rig rotated so that it is oriented vertically with one of its ends resting on the plate at the bottom of the figure. Figure 9 also shows the area where the neutron diffraction measurements are being taken and the line of measurements used to produce the results shown in Figures 11 to 13.

The apparatus shown in Figure 8 can only be used to make measurements on pipe sections such as those on the figure or on very small diameter complete pipes. A full pipe section with a 150 mm diameter can not be bent in this short stressing rig, as the distance

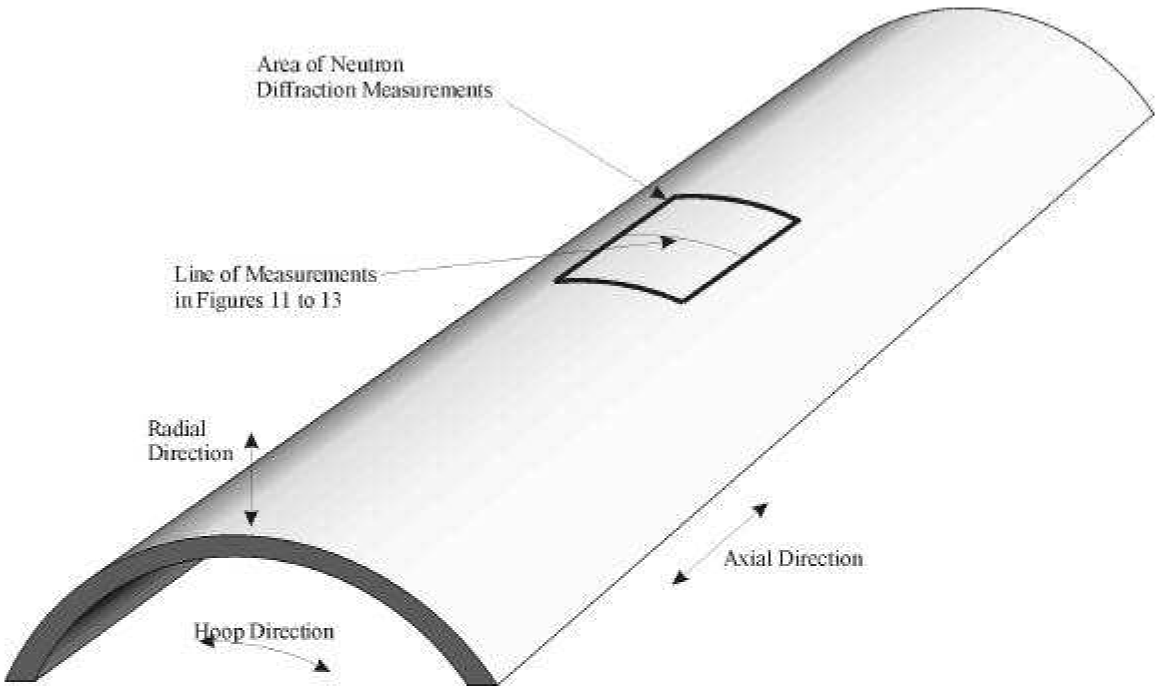

Figure 9 - Direction and location of neutron diffraction measurements

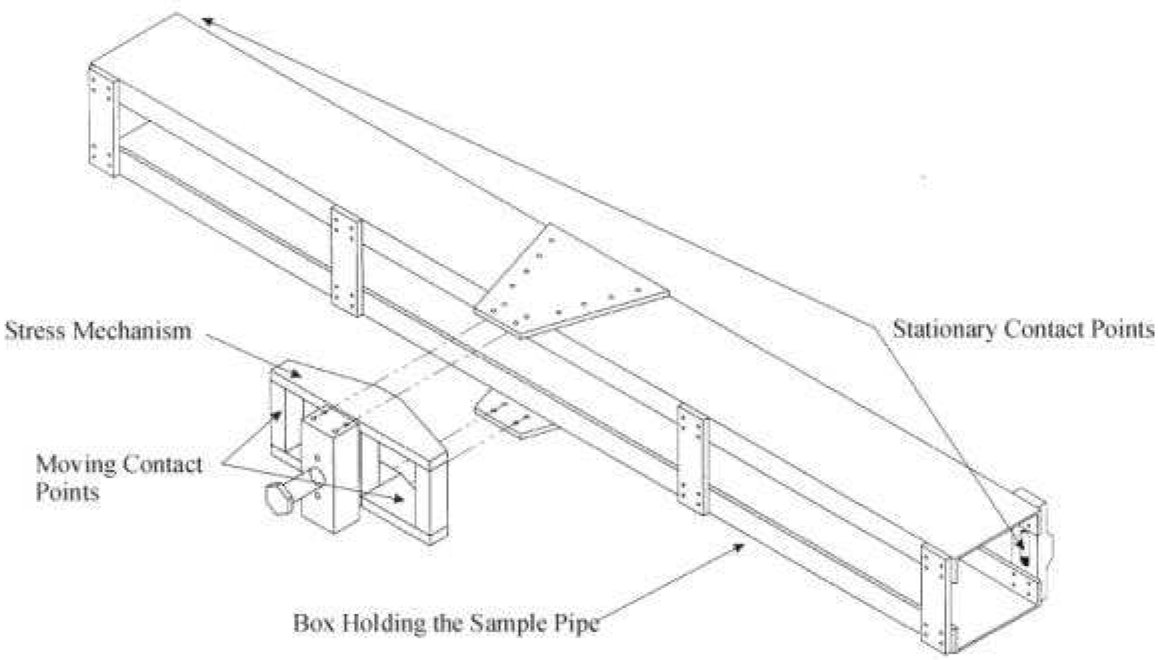

Figure 10 - Long test rig

between the bending points is too short to produce enough bending to break a full pipe section. A 3m (10 ft) long test rig, shown in Figure 10, is being built to allow the bending of full 150 mm diameter pipes. However, measurements on the short rig are still necessary because the maximum length available for making measurements in the radial direction is 610 mm (2 ft). The long test rig will be used to make axial and hoop measurements on the sample, while radial measurements will only be made on samples mounted on the short test rig.

The initial work is being done on pipe sections as shown in Figure 9 in order to investigate the triaxial stress behaviour of grey cast iron in bending. Flat plates or thin strips placed in bending are under biaxial stress conditions, but both full pipe sections and the partial pipe sections used for the first tests are under triaxial stress conditions. Measurements have been made on samples with and without artificially produced corrosion pits. The results of these measurements will be compared to the results of the initial neutron diffraction models to ensure that the modeling is duplicating the real behaviour of the grey cast iron. Upcoming experimental work includes neutron diffraction measurements of small diameter pipes in all three directions on the short test rig, followed by similar measurements in two directions using the long test rig.

4.2 Initial Results

Figures 11 to 13 show neutron diffraction strain measurements taken along the line show in Figure 9 on a pipe section without artificial corrosion pits. These measurements were performed with each end of the pipe section being deflected by 4 mm (0.16 in). The peak in the axial measurements at –3.5 mm thickness and –12 mm hoop position was created by the presence of a natural corrosion pit on the inner surface of the pipe.

The results show that the axial strains are positive in value (the sample was in tension in axial direction), while the radial strains were negative (the sample was in compression in the radial direction) and did not behave in a smooth manner. The hoop strains are negative at the outer surface of the pipe and become positive as they approach the inner surface. Unexpectedly, the results show that the maximum axial strains experienced by the sample are well above the 0.48% ultimate strains measured for the same material under uniaxial tension. The maximum axial strain in tension from the neutron diffraction data (not shown in Figures 11 – 13 and measured when the pipe had been deflected by 5.30 mm (0.21 in), but had still not failed) exceeded 1.05%.

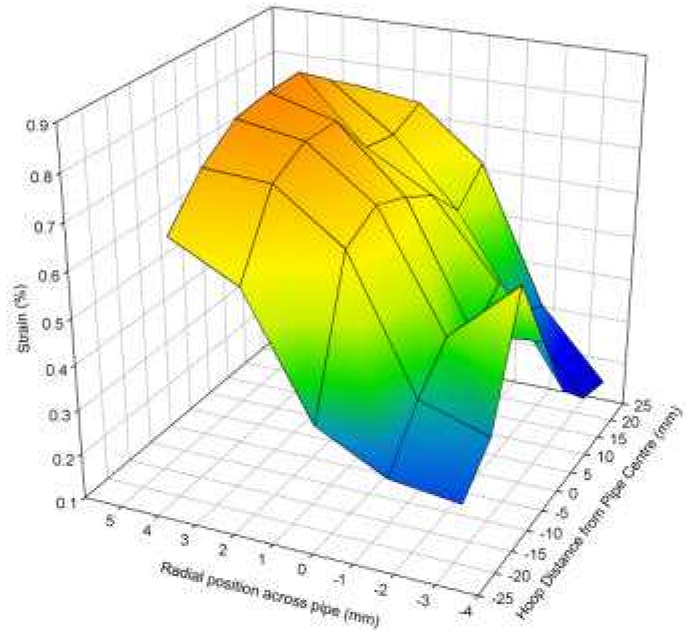

Figure 11 - Axial strains measured across the pipe

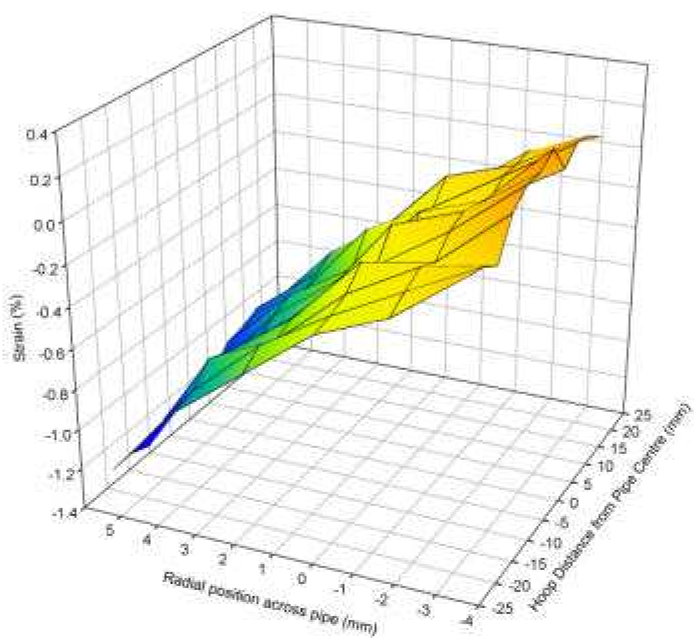

Figure 12 - Hoop strains measured across the pipe

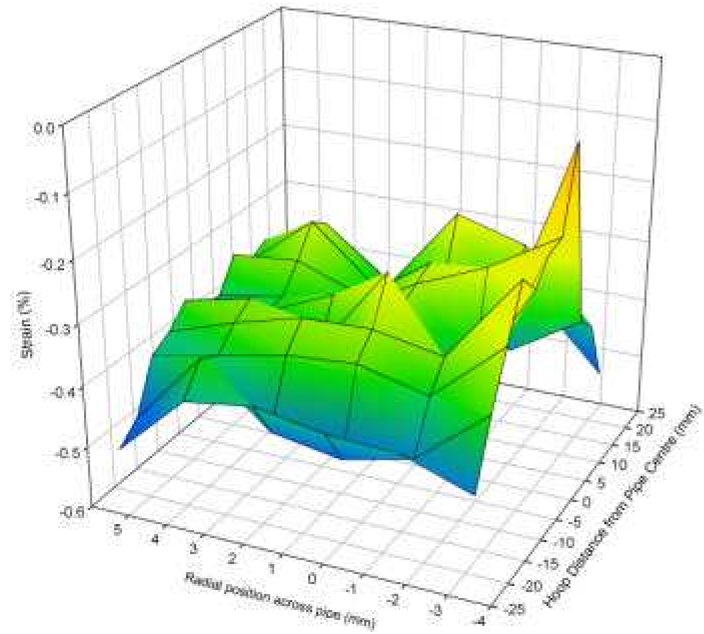

Figure 13 - Radial strains measured across the pipe

This result is unexpected because past work on *bi*axial stress states in grey cast iron (Coffin, 1950; Clough and Shank, 1957; Hjelm, 1994) showed that the ultimate axial strain measured in *uni*axial tension is also the maximum tensile value that a sample can reach in *bi*axial stress, even when one of the two stress axes is in compression while the other is in tension. This behaviour is different from that seen in ductile material such as steel, where shear stress states mean that the ultimate axial strains in uniaxial tension are not those in seen under biaxial stress conditions. The results presented in this paper show that under the *tri*axial conditions experienced by the pipe section, the ultimate tensile strains are different from those produced under uniaxial strain conditions and therefore different from the expected *bi*axial behaviour. The use of the neutron diffraction technique has therefore identified a significant difference between the *tri*axial and the *uni*axial/*bi*axial stress-strain behaviour. This difference will likely prove important to accurately modeling failures in grey cast iron pipes. The results suggest that the strain at failure would likely be underestimated by approximately 100% based on the existing understanding of *bi*axial stress behaviour in grey cast iron, with a corresponding underestimation in the failure stress of approximately 8%.

5 Conclusions

New technologies and engineering procedures have made it possible to determine the amount of corrosion pitting in grey cast iron water mains. This paper has described a research project that investigate how corrosion pits affect the structural strength of those water mains. Combining information from the project and assessments of the extent of corrosion pitting will enable industry practitioners to make better decisions with respect to the replacement and rehabilitation of their water mains. Initial results from the project presented here have given improved guidance on the mechanical testing of cast iron samples from in-service pipes. They have also shown that the triaxial stresses experienced by a pipe in bending may result in different stress-strain and failure behaviour than that which would be expected from past work on uniaxial and biaxial stresses. Future work on the project will confirm these results and provide an improved understanding of the role of corrosion pitting in circumferential failures in gray cast iron pipes.

6 References

ASTM (American Society for Testing Materials), 1994. Standard testing methods for tension testing of metallic materials. ASTM E8-94a. New York.

AWWA, 1939. (American Water Works Association). American Standard Practice for the computation of strength and thickness of Cast-iron pipe. ANSI/AWWA A21.1-39. Denver (1939).

AWWA, 1953. (American Water Works Association). American Standard Practice for the computation of strength and thickness of Cast-iron pipe. ANSI/AWWA A21.1-53. Denver.

Beer, F. P. and Johnston, E. R., 1981. Mechanics of Materials, McGraw-Hill, New York.

Clough, W.R. and Shank, M.E., 1957. The Deformation and Rupture of Gray Cast Iron, Transactions of the American Society for Metals, vol. 49., pp. 241-261.

Coffin, L.F., 1950, The Flow and Fracture of a Brittle Material, Journal of Applied Mechanics, vol. 17, no. 3, pp. 233-247.

Hjelm, H.E., 1994., Yield Surface for Grey Cast Iron Under Biaxial Stress, Journal of Engineering Materials and Technology, vol. 116, no. 2, pp. 148-153.

Makar, J.M. and Chagnon, N., 1999. Inspecting systems for leaks, pits, and corrosion, Journal (American Water Works Association), vol. 91, (7), July, pp. 36-46.

Makar, J.M., Desnoyers, R. and McDonald, S.E., 2001. Failure modes and mechanisms in gray cast iron pipe, Underground Infrastructure Research: Municipal, Industrial and Environmental Applications, Proceedings of the International Conference on Underground Infrastructure Research (Kitchener, Ontario, 6/10/2001), pp. 303-312; M. Knight and N. Thompson, Editors, Swets and Zeitlinger, B.V., Lisse, The Netherlands.

Lu, J. (ed.) 1996, Handbook of measurement of residual stresses / Society for Experimental Mechanics, Inc.; Publisher Lilburn, GA: Fairmont Press (ISBN 088173229X); Upper Saddle River, NJ

Noyan, I. C. and Cohen, J.B. 1987, Residual Stress: Measurement by Diffraction and Interpretation, , Springer-Verlag, 1987 (ISBN: 0-387-96378-2).

Rajani, B.B. and Makar, J.M., 2000. A Methodology to estimate remaining service life of grey cast iron water mains, Canadian Journal of Civil Engineering, 27, (6), December, pp. 1259-1272.

Rajani, B. and McDonald, S., 1995, Water main break data for different pipe materials for 1992 and 1993, Report A-7109.1, Ottawa, Ontario, National Research Council

Talbot, A.N., 1926, Strength Properties of Cast Iron Pipe Made by Different Processes as Found by Tests, Journal of the American Water Works Association, Vol. 16, July, pp.1-44

Walton, C.F. and Opar, T.J., 1981, Iron Castings Handbook, Iron Castings Society, Inc.